Ion pair dissociation of highly excited carbon clusters: size and charge effects

Thibaut Launoy,[1,][*] Karine Béroff,[2,][†] Marin Chabot,[3] Guillaume Martinet,[3]

Arnaud Le Padellec,[4] Thomas Pino,[2] Sandra Bouneau,[3] Nathalie Vaeck,[1]

Jacques Liévin,[1] Géraldine Féraud,[2,][‡] Jérôme Loreau,[1] and Thejus Mahajan[2]

[1]*Laboratoire de Chimie Quantique et Photophysique (CQP) Université*

Libre de Bruxelles (ULB) CP160/09 1050 Bruxelles, Belgium

[2]*Institut des Sciences Moléculaires d'Orsay (ISMO) CNRS-INP*

Univ.Paris-Sud Univ.Paris-Saclay F-91405 Orsay, France

[3]*Institut de Physique Nucléaire d'Orsay (IPNO) CNRS-I2NP3*

Univ.Paris-Sud Univ.Paris-Saclay F-91406 Orsay, France

[4]*Institut de Recherche en Astrophysique et Planétologie*

(IRAP) CNRS-INP Univ.Toulouse 3 F-31028 Toulouse, France

(Dated: July 21, 2016)

We present measurements of ion pair dissociation (IPD) of highly excited neutral and ionized carbon clusters $C_{n=2-5}^{(q=0-3)+}$. The tool for producing these species was a high velocity collision between C_n^+ projectiles (v=2.25 a.u.) and helium atoms. The setup allowed to detect in coincidence anionic and cationic fragments, event by event, leading to a direct and unambiguous identification of the IPD process. Compared to dissociation without anion emission, we found typical 10^{-4} IPD rates, not depending much on the size and charge of the (n,q) species. Exceptions were observed for C_2^+ and, to a lesser extent, C_4^{3+} whose IPDs were notably lower. We tentatively interpreted IPDs of C_2^+ and C_3^+ by using a statistical approach based on the counting of final states allowed by energetic criteria. The model was able to furnish the right order of magnitude for the experimental IPD rates and to provide a qualitative explanation to the lower IPD rate observed in C_2^+.

---

[*] email: tlaunoy@ulb.ac.be

[†] email: karine.beroff@u-psud.fr

[‡] Present address: LERMA, Sorbonne Universités UPMC Univ. Paris 06, Observatoire de Paris, PSL Research University, CNRS F-75252 Paris, France

I. INTRODUCTION

Ion pair dissociation (IPD) is a relaxation process of highly excited molecules proceeding through emission of an anionic and one (or several) cationic fragments. It has been observed long ago in mass spectrometric studies of diatomic molecules [1] and has been mostly studied following photoexcitation by VUV [2, 3] or soft X-ray [4] radiation. IPD was also observed following recombination of low energy electrons with molecular cations, a resonant process competitive with dissociative recombination [5] and also in collisions between molecular ions and atoms in low [6] and high [7–9] velocity collisions. In both cases electronic excitation was assumed to be at the origin of IPD. It is interesting to remark that, even in collisions dominated by nuclear interactions, the anionic production was recently shown to be strongly dependent on electronic excitation and ionization processes [10]. Most of the work on IPD has been devoted to the case of neutral molecules giving rise to one anion and one singly charged fragment. Following the pioneering work of Dujardin et al [11] it was shown that emission of two singly charged fragments or one doubly charged fragment together with one anion was also possible, and was indeed the rule in the case of photoexcitation in inner shells due to the Auger effect [12, 13]. IPD associating three positive charges together with one negative charge has been suspected [14] although never directly identified.

Two formation mechanisms of IPD, direct and indirect, have been proposed. The direct mechanism, population of a state dissociating at infinite internuclear distances towards an ion pair limit, is not expected to be very probable because excitation in the Franck Condon (FC) region has to occur in the repulsive inner wall of the potential energy profile [4]. It is nevertheless possible as recently observed in photoexcitation of O_2 by absorption of three UV photons within a fs laser pulse [15]. The indirect population is expected to occur by coupling between the ion pair state and a highly vibrationally excited Rydberg or cationic states of the molecule populated in the FC region. It was often demonstrated through the observation of vibrational progressions in the fragments spectra [16]. The mechanism may also depend on the dynamics of excitation, i.e. the absorption of one or several photons [16, 17]. In addition to these two mechanisms one has to take into account the crossings between molecular states at large internuclear distances [15] which makes the following of the process very complicated to achieve.

Despite these numerous works there are still many unknowns concerning the IPD process. The yield of IPD is found to vary strongly from one work to another and it is not clear what is governing the obtained values. By the way, this yield is sometimes referenced to the ionization [16], sometimes to the total fragmentation [9] and sometimes to another process [5]. As mentioned before only few

47 works have reported on IPD with three positive charges and no result were obtained, to our
48 knowledge, for four positive charges.

49   In this paper we present measurements of ion pair relaxation of highly excited neutral and
50 ionized carbon clusters $C_{n=2-5}^{q+=0-3}$. The tool for producing these species was a high velocity colli-
51 sion between C_n^+ projectiles ($v = 2.25$ a.u.) and helium atoms. The setup allowed to detect in
52 coincidence anionic and cationic fragments, event by event, leading to a direct and unambiguous
53 identification of the IPD process. To our knowledge these are first results concerning ion pair
54 dissociation of carbon clusters. Moreover we measured ion pair dissociation of carbon clusters in
55 different charge states $q = 0 - 3$ allowing a size and charge effect study to be conducted. In particu-
56 lar, we observed for the first time IPD associated to emission of four positive charges together with
57 one negative charge. Finally we made an attempt to interpret some of IPD rates within a statistical
58 approach. Due to crude approximations this should be seen as a "zero order" interpretation of
59 the results. Still it constitutes a rare case of interpretation of absolute IPD measurements in the
60 literature, to our knowledge.

61   The plan of the paper is as follows. In Section II, we describe the experimental setup and
62 methods used to extract IPD probabilities, namely, coincidence measurements in order to identify
63 the process and target density dependence study to remove contributions from double collisions.
64 In Section III, we present results concerning the IPD probabilities and cross sections for C_n^{q+} as
65 a function of n and q. IPD rates are compared to " normal " dissociation (i.e. without anion
66 emission) and tentatively interpreted, for a part, in Section IV. In Section IV A, the principle
67 of the statistical approach is presented and applied to C_2^+ and C_3^+ in Sections IV B - IV D. We
68 conclude in Section V.

II. EXPERIMENT

70   The experiment has been performed at the Tandem accelerator in Orsay using the AGAT
71 setup. The setup is the same as the one described in [18]. Briefly , C_n^+ projectiles of 125 keV/u
72 energy (constant velocity 2.25 a.u.) were delivered by the accelerator and sent to the AGAT setup
73 consisting of a collision chamber, a fragment's electrostatic analyser and a fragment's detection
74 chamber. In the collision chamber, the C_n^+ projectiles were traversing a low density helium gaseous
75 jet whose thickness, nδx, could be varied by changing the flow rate through the formation capillary
76 [19]. In the electrostatic analyser chamber, projectiles and fragments were deflected according to
77 their charge over mass ratios thanks to the application of a strong electric field of a few tens of
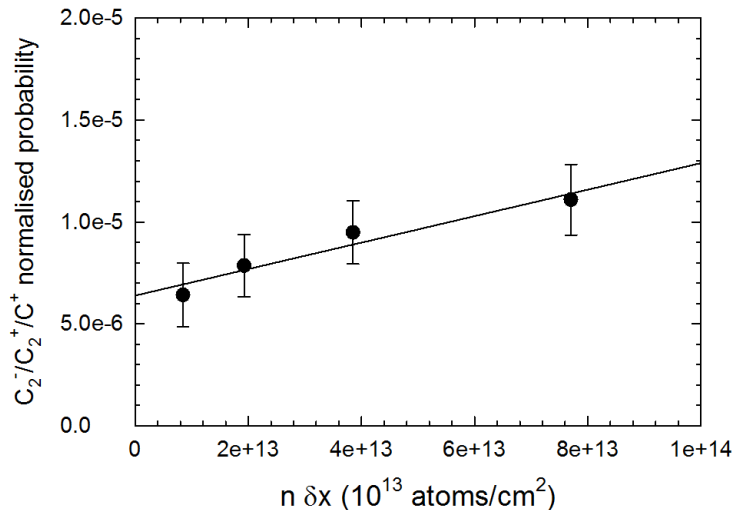
FIG. 1. Normalised ion pair dissociation probability along the $C_2^-/C_2^+/C^+$ channel as a function of the helium target thickness (collision at 2.25 a.u. for $C_5^+ - He$)

78 kV/cm produced between two parallel plates. In the detection chamber six or seven solid state

79 silicon detectors were positioned as to intercept negatively charged, neutral and positively charged

80 fragments. The current signals issued from the detectors were used to extract the masses of the

81 fragments and allowed to resolve pile up events associated to the impact of numerous fragments in

82 the same detector (case of the neutral fragments detector for instance [20]). With these methods all

83 fragments were detected (100% efficiency, 4π detection in the projectile frame) and identified with

84 respect to their mass and charge. In some of the experiments the detector of neutral fragments

85 was replaced by an original position sensitive CCD camera [21]. With this detector, we extracted

86 the dissociative kinetic energy of the C fragment following dissociation of C_2^{q+} into C^{q+}/C [22].

87   Whereas typical target thicknesses (few 10^{13} atoms/cm^2) guaranteed the single collision condi-

88 tion for all major processes (electronic excitation, ionization, single electron capture) this was not

89 the case for processes of very small cross sections such as double electron capture [18] and ion pair

90 dissociation. In this last case, we proceeded as explained in [18] i.e. by plotting the target thick-

91 ness dependence of the process of interest, normalised to a linearly dependent reference process

92 (often the sum of electronic excitation, ionization and electron capture). Figure 1 is illustrating

93 the method in the case of the $C_2^-/C_2^+/C^+$ IPD process recorded in the $C_5^+ - He$ collision. The

94 probability of the IPD process in a single collision is extracted from the normalised probability

95 obtained at zero thickness.

III.   EXPERIMENTAL RESULTS FOR ION PAIR PROBABILITIES AND CROSS SECTIONS

A.   Measured ion pair dissociation probabilities and cross sections

In Table I are reported measured IPD probabilities normalised to the total fragmentation probability of the C_n^{q+} species for $n = 2 - 5$ and $q = 0 - 3$. Also reported are the Branching Ratios (BR) for IPD in the various ion pair channels and the energetical cost of each channel i.e. the minimum energy that has to be deposited in the C_n^{q+} species as to reach the considered channel. This last quantity was extracted from the theoretical works of Diaz-Tendero and collaborators on C_n^{q+} clusters [23, 24] using electron affinities of C_n^- [25] and assuming no barriers to the dissociation [26].

It is readily seen that the IPD process is a very small part of the total dissociation probability (with a probability ranging between 10^{-5} to a few 10^{-4}), this last one being essentially without anionic emission (referred in the paper as to the " normal " dissociation). It is also seen that the energetical cost of the process is high, from 15 eV up to 38 eV depending on the system and on the channel. The more probable ion pair channels are usually not the ones reachable with the lowest energy. For instance three-fragments channels are more probable than two-fragments channels for $q = 0$ and $n = 4 - 5$ whereas four-fragments channels are more probable than three-fragments channels for $q = 1$ and $n = 4 - 5$. This indicates that IPD involves highly excited states. On the other hand, some molecular anions are detected, in particular the molecular anion C_2^- which was prominent in the fragmentation of negatively charged carbon clusters C_n^- [18].

In Figure 2, are presented measured IPD cross sections of C_n^{q+} clusters as a function of the cluster size n and for various values of q ($q = 0$ to $q = 3$ from top-left to bottom-right panel of Figure 2). These values were obtained by summing IPD probabilities for each (n,q) species and using measured values of the reference cross sections. It is seen that most of the IPD cross sections are around a few 10^{-20} cm^2 with some notable exceptions for C_2^+ ($2.9\,10^{-21}$ cm^2) and C_4^{3+} ($8.6\,10^{-21}$ cm^2). IPD cross sections from multicharged species (q$\geqslant$2) are relatively large as compared to q=0 and q=1. This was unexpected. In fact IPD cross sections of C_n^{q+} species are more or less following the cross sections for production of the species. Since C_n^{q+} species with q$\geqslant$2 are mainly fragmenting this result may be understood by assuming that IPD is a constant percentage of the dissociation, as discussed below.

n,q	Channel	Ion pair dissociation probability (abs.err)	Branching ratio within ion pair dissociation (abs.err)	Energy above the ground state of C_n^{q+}(eV)
2,0	C^-/C^+	$5.43(0.65)10^{-4}$	1	16.1
2,1	C^-/C^{2+}	$2.94(1.62)10^{-5}$	1	28.5
3,0	C_2^-/C^+	$4.29(0.53)10^{-4}$	0.58(0.07)	15.7
	$C^-/C^+/C$	$1.91(0.50)10^{-4}$	0.26(0.07)	23.9
	C^-/C_2^+	$1.20(0.32)10^{-4}$	0.16(0.04)	18.2
3,1	$C^-/2C^+$	$2.90(0.2)10^{-4}$	1	23.2
4,0	$C^-/C_2/C^+$	$6.10(3.5)10^{-5}$	0.36(0.21)	22.9
	$C_2^-/C/C^+$	$5.07(3.3)10^{-5}$	0.30(0.19)	20.9
	C_2^-/C_2^+	$3.47(2.0)10^{-5}$	0.20(0.12)	15.5
	C_3^-/C^+	$2.40(2.0)10^{-5}$	0.14(0.12)	14.6
4,1	$C^-/C/2C^+$	$1.53(0.22)10^{-4}$	0.53(0.07)	28.5
	$C^-/C_2^+/C^+$	$7.09(1.3)10^{-5}$	0.25(0.04)	23.0
	$C_2^-/2C^+$	$6.33(1.19)10^{-5}$	0.22(0.04)	20.4
4,2	$C^-/3C^+$	$1.57(0.14)10^{-4}$	0.96(0.01)	22.4
	$C^-/C^{2+}/C^+/C$ [b]	$6.0(0.6)10^{-6}$	0.04(0.01)	35.5
4,3	$C^-/2C^+/C^{2+}$ [b]	$7.31(2.12)10^{-5}$	0.96(0.03)	38.1
	$C^-/C/2C^{2+}$ [b]	$2.58(2.05)10^{-6}$	0.04(0.03)	39.9
5,0	C_2^-/C_3^+	$4.5(2.0)10^{-5}$	0.42(0.16)	14.5
	$C_2^-/C_2/C^+$	$3.6(1.5)10^{-5}$	0.31(0.13)	21.0
	$C_2^-/C_2^+/C$	$3.2(1.5)10^{-5}$	0.27(0.13)	21.8
5,1	$C_2^-/2C^+/C$	$5.78(0.97)10^{-5}$	0.30(0.05)	28
	$C^-/2C/2C^+$	$5.67(1.11)10^{-5}$	0.29(0.06)	36
	$C^-/C/C^+/C_2^+$	$2.91(0.8)10^{-5}$	0.15(0.04)	30.3
	$C_2^-/C_2^+/C^+$	$2.33(0.5)10^{-5}$	0.12(0.03)	22.5
	$C^-/C_2/2C^+$	$2.0(0.6)10^{-5}$	0.10(0.03)	30
	$C_3^-/2C^+$	$8.0(3.2)10^{-6}$	0.04(0.02)	21.1
5,2	$C^-/C/3C^+$	$1.56(0.24)10^{-4}$	0.67(0.10)	31
	$C_2^-/3C^+$	$3.96(0.77)10^{-5}$	0.17(0.03)	21.7
	$C^-/C_2^+/2C^+$	$3.59(0.77)10^{-5}$	0.16(0.03)	25.4
5,3	$C^-/4C^+$	$2.31(0.26)10^{-4}$	1	17.6

[a] measurements performed at v=2.6 a.u.

TABLE I. Measured ion pair probabilities in individual channels of C_n^{q+}, normalised to the total dissociation probability of the species.
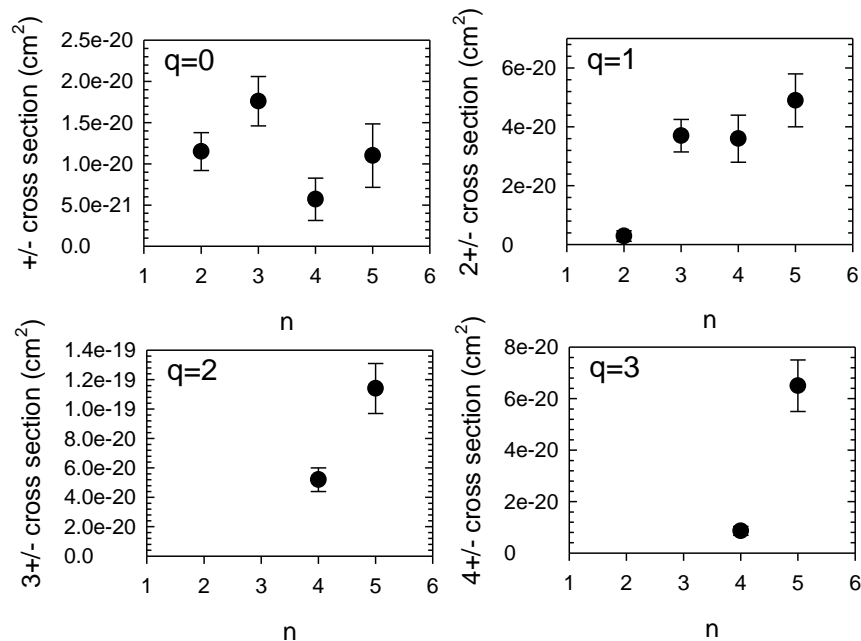
FIG. 2. Measured ion pair dissociation cross sections of C_n^{q+} clusters as a function of n (abscissa) and for various q values (from top-left to bottom-right q=0,1,2,3)

.

B. Ion pair dissociation rates as compared to the total dissociation of a C_n^{q+} species

We compare, within a given (n,q) species, the total IPD probability to the total dissociation probability. Results, obtained by summing all individual channels IPD probabilities of Table I are displayed in Figure 3. It is seen that the rates are not depending much on the cluster size and charge except the two channels already remarked as particularly low : C_2^+ and, to a lesser extent, C_4^{3+}. The difference between the IPD of C_2^+ and C_3^+ (more than a factor 10) is particularly
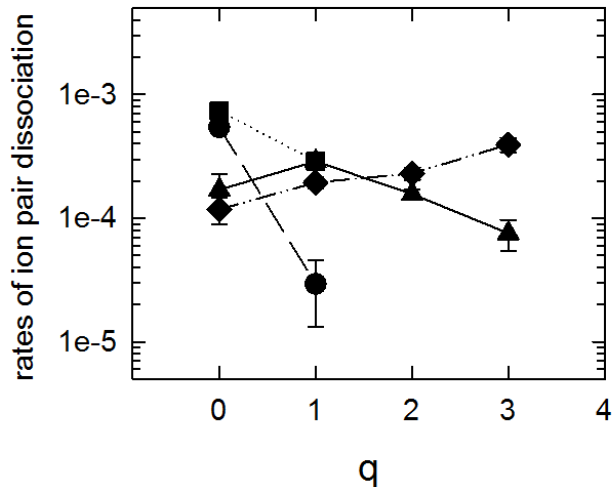
FIG. 3. Measured rates of ion pair dissociation as compared to total dissociation of C_n^{q+} species as a function of q and for various n values : circles, squares, triangles up, diamonds for n=2,3,4,5 respectively. Lines are to guide the eye.

remarkable and is analysed below.

IV.   TENTATIVE INTERPRETATION OF IPD IN C_2^+ AND C_3^+

As mentioned before the IPD process is complex and may occur through various mechanisms taking place at various internuclear distances R. For instance, in the case of C_2^+, the avoided crossings that are taking place at large internuclear distances between ion pair states (shown by the dashed-dotted lines [27]) and molecular states dissociating into C / C^+ are shown in Figure 4. The potential energy curves have been calculated with multi-configurational *ab initio* methods (CASSCF/MRCI+Davidson correction with a cc-pVTZ basis set using the MOLPRO package [28], to be published). The complexity of the molecular structure and the highly excited states involved make a quantitative study and following of the IPD process impossible to handle. On the other hand, when many events with different characteristics (energy and type of the populated molecular state, mechanism at play) are summed and averaged as it is done in the experiment, another approach relying on statistics is possible. Our approach, explicited below, is mainly based on energetic criteria and the counting of open final channels that are supposed to be all equiprobable.
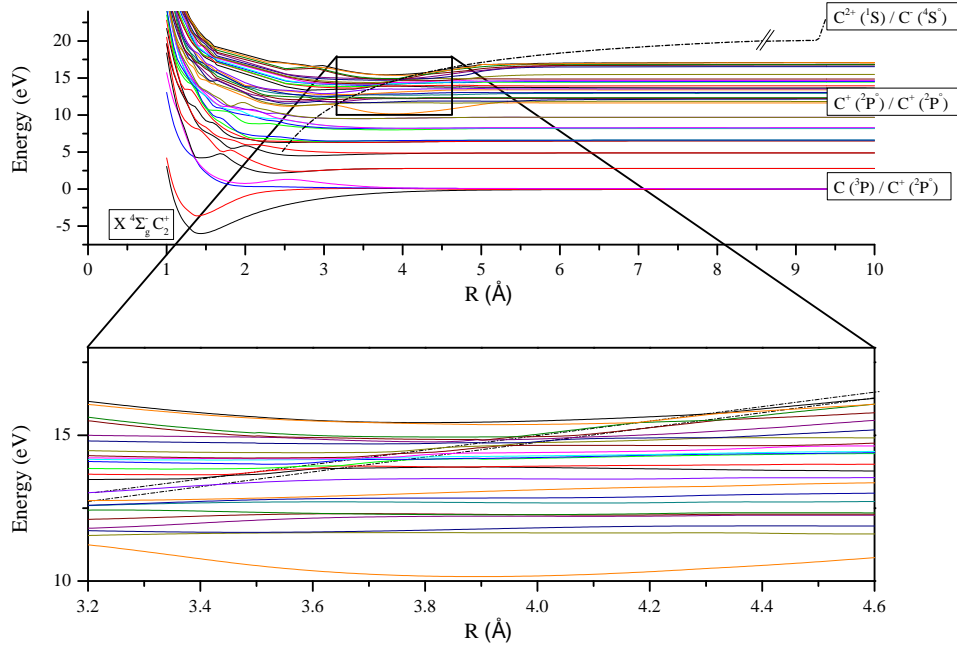
FIG. 4. (Color on line) Visualization of avoided crossings between highly excited $^4\Sigma^-$ states of C_2^+ and the two ion pair states correlating to the C^{2+}/C^- ion pair channel (dashed-dotted lines on the lower panel). The upper panel shows the PECs (in eV) of the low-lying molecular states of C_2^+. Lower energy dissociation limits for C/C^+, C^+/C^+ and C^{2+}/C^- are also reported.The calculations were performed from 10.0 Å to 1.0 Å with steps of 0.01 Å except near avoided crossings where the step was 0.001 Å.

A. Expression of the IPD rate

The experimental results to be interpreted are the rates of ion pair dissociation as compared to the " normal " dissociation, namely, $R_2 = \frac{p(C^{2+}/C^-)}{p(C/C^+)}$ for C_2^+ et $R_3 = \frac{p(C^+/C^+/C^-)}{p(C^+/C/C)}$ for C_3^+. As we do not know by which mechanism the ion pair states are populated (direct or indirect process or through crossings at large internuclear distances), we will make our reasoning mainly by using energetic criteria. In particular dissociation into an ion pair is open for any state situated energetically above the first ion pair dissociation channel, named Ion Pair Threshold (IPT), equal to 28.5 eV for C_2^+ and 23 eV for C_3^+. On the other hand, fragmentation of C_2^+ and C_3^+ clusters into normal dissociation is open as long as the internal energy E* is larger than the first dissociative channel (E_{diss}) equal to 5.4 eV for (C/C^+) and 12 eV for ($C^+/C/C$). We may then write :

$$R = \frac{\int_{IPT}^{\infty} BR(E^*)\frac{d\sigma}{dE^*}dE^*}{\int_{E_{diss}}^{IPT} \frac{d\sigma}{dE^*}dE^* + \int_{IPT}^{\infty} \frac{d\sigma}{dE^*}(1 - BR(E^*))dE^*} \tag{1}$$

156 where $\frac{d\sigma}{dE^*}$ is the differential in internal energy E^* dissociative excitation cross section and
157 BR(E^*) is the ion pair branching ratio, i.e. the probability that a molecular state situated in this
158 energy domain [IPT-∞] dissociates into an ion pair limit. We introduce the dissociative electron
159 excitation cross section σ :

$$\sigma = \int_{E_{diss}}^{\infty} \frac{d\sigma}{dE^*} dE^*, \tag{2}$$

160 and the internal energy distribution due to dissociative excitation f(E^*) :

$$f(E^*) = \frac{\frac{d\sigma}{dE^*}}{\sigma}, \tag{3}$$

161 so that we can express R as :

$$R = \frac{A}{1-A} \tag{4}$$

162 with :

$$A = \int_{IPT}^{\infty} f(E^*) BR(E^*) dE^*. \tag{5}$$

163 ## B. Internal energy distributions f(E^*) of C_2^+ and C_3^+

164 In C_2^+ and C_3^+ IPD is likely to arise from relaxation of electronically excited clusters in the
165 valence shell. Indeed excitation in inner shell, of much smaller cross section (around 10^{-18} cm^2 per
166 carbon atom [29]), is followed in 99.8% of the cases [29] by a rapid Auger effect of lifetime around
167 a few fs [30] i.e. before dissociation occurs [12, 13]. The internal energy distributions of C_2^+ and C_3^+
168 due to dissociative electronic excitation in valence shells have been calculated using an Indepen-
169 dent Atom and Electron (IAE) model [31] together with Classical trajectory Monte Carlo Method
170 (CTMC) for the calculation of the energy deposited in individual C and C$^+$ atoms. More details
171 are given in references [32] and [33]. In particular, we showed [32] that the obtained internal energy
172 distributions allowed to reproduce the measured branching ratios of dissociation of C_n^+ clusters. In
173 Figure 5 are shown f(E^*) obtained for C_2^+ and C_3^+ within this simple model. Structures are roughly
174 associated to excitation of $2p$ electrons (lower energy peak), $2s$ electrons (middle ones) and double
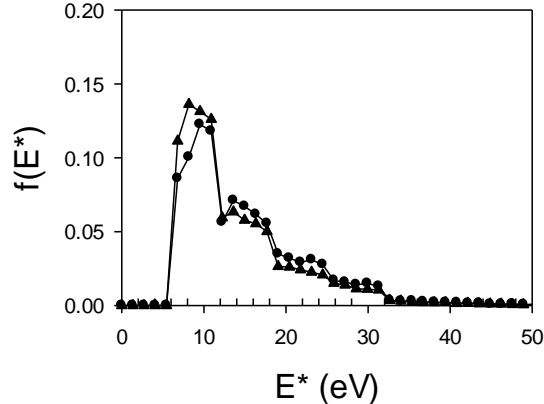
FIG. 5. Internal energy distribution of excited C_2^+ (circles) and C_3^+ (triangles) calculated with the IAE model.

excitation (above 18 eV). It is readily seen that the part of excitation allowing dissociation into the ion pair ($E^* \geqslant$ IPT) is small, roughly 7% for C_2^+ (IPT = 28.5 eV) and 13% for C_3^+ (IPT = 23.1 eV).

There are constraints about the molecular states that are populated during the collision. If we assume that dipole transitions dominate, which is indeed the case in high velocity collisions [34], transitions from the initial molecular states must obey the following selection rules for linear molecules [35, 36]: $\Delta S = 0$ (spin conservation), $\Delta \Lambda = 0, \pm 1$ (Λ is the projection along the internuclear distance axis of the electronic orbital angular momentum), u $\leftrightarrow$ g transition (symmetry with respect to the molecule symmetry center), $\Sigma^+ \leftrightarrow \Sigma^-$ forbidden (symmetry with respect to a plane containing R). Starting from the C_2^+ ground state (X $^4\Sigma_g^-$) we populate final states of the $^4\Sigma_u^-$ and $^4\Pi_u$ symmetry whereas populated states from the C_3^+ ground state (X $^2\Sigma_u^+$) are of the $^2\Sigma_g^+$ and $^2\Pi_g$ types.

C. Branching ratios towards ion pair dissociative channels BR(E^*)

Dissociation of molecular states depends strongly on the considered state. As seen in Figure 4 highly excited molecular states tend to correlate, adiabatically, to highly excited dissociative limits. Considering non adiabatic transitions a much higher range of dissociation limits is open as all dissociative limits situated below E^* are potentially reachable.

Indication of population of low energy dissociative channels is furnished from the measurement of the Kinetic Energy Release (KER) of C_2^+ (see experimental part). Indeed a peak at 3 eV was experimentally obtained that roughly corresponds to the more probable deposited energy

195 (10 eV) from which is subtracted the lowest energy dissociation channel $C^+(GS) - C(GS)$ (5.4

196 eV). Within the frame of our statistical approach we assumed in the following analysis that all

197 dissociative limits were equally populated. This is a crude approximation, but better knowledge

198 concerning dissociation of highly excited molecules is not available. Then, we can relate the ion

199 pair branching ratio to the relative number of ion pair dissociation limits as compared to the total

200 number of dissociative channels. On the other hand, the number of molecular states connected to a

201 given dissociation limit also matters. We then defined $BR(E^*)$ as the ratio between the number of

202 molecular states connected to ion pair limits divided by the number of molecular states connected

203 to all other dissociative channels. Expressions of $BR(E^*)$ in C_2^+ and C_3^+ are given in Eq. (6) and

204 (7) respectively. In these expressions molecular states to be considered are those allowed by dipole

205 transitions from the initial state, as discussed before. The E^* dependence of $BR(E^*)$ comes from

206 the fact that the number of dissociative channels situated below E^* obviously depends on E^*.

$$BR(E^*) = \frac{N_{mol.states} \to C^{2+}/C^-}{N'_{mol.states} \to C^+/C} \tag{6}$$

207   for the case of C_2^+ dissociation and

$$BR(E^*) = \frac{N_{mol.states} \to C^+/C^+/C^-}{N'_{mol.states} \to C^+/C/C} \tag{7}$$

208   for the case of C_3^+ dissociation.

209

210   The first task for calculating $BR(E^*)$ is to count the number of dissociative channels situated

211 below E^* ($E^* \geq IPT$) and above E_{diss}. These channels associate various C and C^+ terms ($^{2S+1}L_{u,g}$)

212 a list of which can be found for instance in the NIST database [37]. One difficulty associated to the

213 large $\Delta = (E^* - E_{diss})$ domains that have to be considered ($\Delta_{min} = 10$ eV in C_3^+ and $\Delta_{min} = 23.1$

214 eV in C_2^+) is that an infinite number of dissociative states are theoretically to be introduced as

215 long as $\Delta \geq 11.26$ eV (Rydberg states $2p \to nl$ in C) and $\Delta \geq 24.38$ eV (Rydberg states in C^+).

216 It is nevertheless expected that contribution of high n values will decrease with n. Schiavone et

217 al [38] have shown for instance that the production of high-Rydberg (HR) atomic fragments in

218 electron-impact dissociation of 13 molecules was following a $\frac{1}{n^3}$ dependence. These measurements

219 were performed at 100 eV electron kinetic energy ($v_p = 2.7$ a.u.), a collision system very close from

220 ours according to the Z_p/v_p criterium ($v_p = 2.25$ a.u. and $Z_p(He)=1$-2 depending on the impact

221 parameter in the here studied systems). Since molecular Rydberg states are possibly contributing

to the ion pair dissociation and since molecular Rydberg states are likely to dissociate into HR atomic fragments [39] the question arises where to cut in n the countings. The IPD process representing roughly 10^{-4} of the dissociative excitation cross section we see from the $\frac{1}{n^3}$ law that HR atomic fragments with n up to $n=60$ could be considered. In the NIST database terms up to $n=30$ are typically included. In order to see the effect of the cut in n, we also made countings with $n=20$ and $n=10$.

The second task is to calculate the number of molecular states correlating to the various dissociation limits. For that we used the building-up principles given in Herzberg (1950) [35] for diatomics and Herzberg (1966) [36] for polyatomics. For C_2^+ the counting is rather straightforward using the Herzberg Tables whereas the counting for C_3^+ is more complicated due to the permutation of the three identical carbon nuclei, see the Appendix. The effect of the permutation has been taken into account exactly for the calculation of the number of ion pair molecular states entering in the numerators of Eq. (6) and Eq. (7) (and reported in Table II and Table III). The counting of states entering in the denominators of Eq.(6) and Eq. (7) strictly follows the group theoretical treatment illustrated in the Appendix for ion pair channels. This leads to the introduction of multiplication factors resulting from permutational symmetry. For C_3^+, most of the $C^+/C/C$ channels correspond to the case where both C atoms are in a different electronic state, which implies that a permutational multiplication factor of 3 applies to g or u selected states. Neglecting the occurrence of the rare channels in which both C atoms are in the same state, one can adopt the factor of 3 as a mean value for all molecular states emerging from $C^+/C/C$ dissociation limits. Associated values are reported in Table IV and Table V. As an example, in C_2^+, the lower dissociation limit for the normal dissociation is $C^+(^2P^o)$ - $C(^3P)$ to which 24 molecular states are connected of the $^{2,4}\Sigma_{u,g}^+$, $^{2,4}\Sigma_{u,g}^-$, $^{2,4}\Pi_{u,g}$ and $^{2,4}\Delta_{u,g}$ types. According to the dipole transition rules only $^4\Sigma_u^-$ and $^4\Pi_u$ states should be considered when starting from C_2^+ (X $^4\Sigma_g^-$).

D.   IPD rates in C_2^+ and C_3^+, comparison with experiment and discussion

We give in Table II and Table III the ion pair dissociation limits which are in the energy domain between threshold and 35 eV together with the number and type of molecular states which are converging to these limits and are possibly populated according to the dipole selection rules. For C_2^+ (see Table II) we also made the counting starting from the $a^2\Pi_u$ metastable state since this state is likely to be present in the incoming beam [40] and since it leads to a very different IPD

Dissociation limits	Energy above C_2^+ $(X^4\Sigma_g^-)$(eV)	Molecular states (number)
$C^-(^4S^\circ) - C^{2+}(^1S)$	28.5	$^4\Sigma_u^-$ (1)
$C^-(^4S^\circ) - C^{2+}(^3P^\circ)$	35.0	$^4\Sigma_u^-$ (1), $^4\Pi_u$ (1)
	34.2 (above C_2^+ $(a^2\Pi_u)$)	$^2\Sigma_g^-$ (1), $^2\Pi_g$ (1) (from C_2^+ $(a^2\Pi_u)$)

TABLE II. Ion pair dissociation limits situated in the 28.5-35 eV energy domain above the ground state of C_2^+. The number and type of molecular states converging to each limit and meeting the selection rules (see text and appendix) are given in the last column. The number of states of each type is given in parenthesis. For the second ion pair limit, molecular states populated from the metastable C_2^+ $(a^2\Pi_u)$ are also reported.

253 rate. Indeed, due to spin conservation, the first ion pair dissociation limit cannot be reached from
254 C_2^+ $(a^2\Pi_u)$ and only the second one, much higher in energy, can be populated.

255   In contrast with these few ion pair dissociation limits, the number of final states associated to
256 a " normal " dissociation (of the C^+ / C type for C_2^+, on the C^+ / C / C type for C_3^+) is enormous
257 (see Table IV and Table V). On the basis of the NIST database, we identified 400 C^+ / C limits
258 situated below IPT = 28.5 eV to which converge more than 1500 allowed molecular states; this
259 number is doubled at E* = 35 eV. For the case of C_3^+, the number of final dissociative states of
260 the C^+ / C / C type is more than 200 at E* = 23 eV and close to 30000 at E* = 35 eV. This very
261 large jump between E*=23 eV and E*=35 eV is due to the fact that, at the latter energy, two
262 Rydberg series associated to the two carbon atoms contribute to the number of dissociative limits.
263 Considering now the cuts at $n=20$ and $n=10$ we find a moderate effect in C_2^+ whereas the larger
264 effect is seen in C_3^+ at E*=35 eV, originating from the double cut on the two Rydberg series. But
265 the overall effect on the IPD rate remains small because this energy does not contribute much.
266

267   On the basis of these countings, BR(E*) (formulae (6) and (7)) were calculated for three E*
268 values : 28.5 eV, 33.5 eV and 35 eV for C_2^+ (BRs respectively equal to 6.6 10^{-4}, 4.1 10^{-4} and 9.7
269 10^{-4}), 23 eV, 28.5 eV and 35 eV for C_3^+ (BRs respectively equal to 4.6 10^{-4}, 7.1 10^{-4} and 4.0
270 10^{-5}). The rates were then obtained using equations (4) and (5) where integration per parts was
271 made over the three values of E*. From f(E*) we get for the A values of C_2^+ (Eq.(8) and Eq. (9))
272 and C_3^+ (Eq. (10)):

Dissociation limits	Energy above C_3^+ $(X^2\Sigma_u^+)$(eV)	Molecular states (number)
$C^-(^4S^\circ) - C^+(^2P^\circ) - C^+(^2P^\circ)$	23	$^2\Sigma_g^+$ (1), $^2\Pi_g$ (3)
$C^-(^4S^\circ) - C^+(^2P^\circ) - C^+(^4P)$	28.5	$^2\Sigma_g^+$ (12), $^2\Pi_g$ (12)
$C^-(^4S^\circ) - C^+(^2P^\circ) - C^+(^2D)$	32.5	$^2\Sigma_g^+$ (3), $^2\Pi_g$ (9)
$C^-(^4S^\circ) - C^+(^4P) - C^+(^4P)$	33.6	$^2\Sigma_g^+$ (3), $^2\Pi_g$ (6)
$C^-(^4S^\circ) - C^+(^2P^\circ) - C^+(^2S)$	35	$^2\Sigma_g^+$ (0), $^2\Pi_g$ (3)

TABLE III. Same legend as Table II for C_3^+

	N_{diss} 28.5 eV	N_{diss} 35 eV	N_{mol} 28.5 eV	N_{mol} 35 eV
NIST	400	916	1508	3100
$n \leq 20$	383	880	1408	2955
$n \leq 10$	304	708	1206	2311

TABLE IV. Normal dissociation in C_2^+ : Number of dissociative states of the C^+/C type (N_{diss}) situated below 28.5 eV (column 2) and below 35 eV (column 3) as a function of the cut in n (see text). In column 4 and 5 are reported the number of molecular states converging to these limits and allowed by selection rules.

$$A(X^4\Sigma_g^-) = 0.03 * (\frac{BR(28.5) + BR(33.5)}{2}) + 0.02 * (\frac{BR(33.5) + BR(35)}{2}) \qquad (8)$$

	N_{diss} 23 eV	N_{diss} 35 eV	N_{mol} 23 eV	N_{mol} 35 eV
NIST	226	26767	8631	1303374
$n \leq 20$	226	23335	8631	1000608
$n \leq 10$	226	13594	8631	572085

TABLE V. Normal dissociation in C_3^+ : Number of dissociative states of the $C^+/C/C$ type (N_{diss}) situated below 23 eV (column 2) and below 35 eV (column 3) as a function of the cut in n (see text). In column 4 and 5 are reported the number of molecular states converging to these limits and allowed by selection rules.

$$A(a^2\Pi_u) = 0.02 * BR(35) \tag{9}$$

$$A(X^2\Sigma_u^+) = 0.07 * \left(\frac{BR(23) + BR(28.5)}{2}\right) + 0.04 * \left(\frac{BR(28.5) + BR(35)}{2}\right) \tag{10}$$

Results for the calculated rates and comparison with the experimental rates are given in Table VI.

Initial state	Calculated IPD Rate NIST	Calculated IPD Rate $n \leq 20$	Calculated IPD Rate $n \leq 10$	Experimental IPD Rate (rel.error)
C_2^+ (X $^4\Sigma_g^-$)	$3.0 \ 10^{-5}$	$3.2 \ 10^{-5}$	$3.9 \ 10^{-5}$	$3.0 \ 10^{-5}$ (60%)
C_2^+ ($a^2\Pi_u$)	$8.7 \ 10^{-6}$	$9.0 \ 10^{-6}$	$1.1 \ 10^{-5}$	
C_3^+ (X $^2\Sigma_u^+$)	$5.6 \ 10^{-5}$	$5.9 \ 10^{-5}$	$7.0 \ 10^{-5}$	$5.3 \ 10^{-4}$ (30%)

TABLE VI. Comparison between measured and predicted by the model rates for ion pair dissociation. Experimental rates are those of Figure 3 whereas modelled rates are calculated with equations (4) and (5).

As seen from Table VI the model furnishes the right order of magnitude for the IPD rates. This means that the relative number of accessible ion pair dissociative limits is indeed important in this matter. The very good agreement between the model and the experimental result for C_2^+ (X $^4\Sigma_g^-$) is probably accidental because we do not expect the model to be so accurate. Relative values are more meaningful. We note that the IPD rates are not dependent much on the cut in n. For C_2^+ we have a sizeable lowering of the rate when considering the molecule in a metastable state instead of in the ground state but unfortunately the experimental contribution of the former one is unknown. We observe that predicted IPD rates are larger in C_3^+ than in C_2^+, as in the experiment. This results can be explained by two factors. First, the density of ion pair states is much smaller in C_2^+ than in C_3^+ (factor 15 in the [28.5, 35]eV energy domain) ; this will play a role for instance in the [33.5, 35] eV range in C_2^+ where there is no ion pair limit at all. Second, the IPT value is much higher in C_2^+ (28.5 eV) than in C_3^+ (23 eV). This energetical cost reduces roughly by a factor 2 the excitation probability above IPT in C_2^+ as compared to C_3^+, on the basis of the f(E*)

289 function. Both phenomena have their origin in the fact that a C^{2+} fragment is emitted in IPD of
290 C_2^+ and not in IPD of C_3^+. The same explanation is probably at the origin of the lower IPD rate
291 for C_4^{3+} as compared to C_5^{3+} (see Table I).

292

V.   CONCLUSION AND PERSPECTIVES

294   In conclusion, we have measured, for the first time, the ion pair dissociation cross sections
295 of carbon clusters C_n^{q+} of various masses ($n = 2 - 5$) and charges ($q = 0 - 3$). Highly excited
296 and ionized species were formed by high velocity collisions between C_n^+ clusters and helium atoms
297 ($v = 2.25$ a.u., $n = 1 - 5$). By performing coincidences between anionic and cationic fragments
298 it was possible to resolve all ion pair dissociation channels of a given (n,q) species. As compared
299 to normal dissociation without anionic emission, it was found that the small IPD rates (of the
300 order of 10^{-4}) were almost constant with n and q with the notable exception of C_2^+ giving rise to
301 C^{2+} / C^- fragments about ten times smaller than the IPD of C_3^+ giving C^+ / C^+ / C^- fragments.
302 We tentatively interpreted C_2^+ and C_3^+ IPD rates by applying a statistical model based on the
303 main approximation that these rates are proportional to the relative number of open ion pair
304 dissociative channels at infinite distances. Despite crude approximations, in particular the use of
305 internal energy distribution of C_n^+ clusters obtained with a simple model and the assumption of
306 equal population for all energetically open dissociative limits, it was possible to find the right order
307 of magnitude for the IPD rates in C_2^+ and C_3^+ and to explain qualitatively the lower value obtained
308 in the former case.

309   As to perspectives, the question arises whether a similar model could be applied to interpret
310 results of the other clusters. Considering first the size and keeping q=1 we are confronted to a
311 number of states to be considered which becomes enormous and, at the light of results obtained on
312 C_3^+, probably too large. With that respect it would help to go beyond the assumption of equally
313 probable dissociative channels. This would imply to find some propensity rules applicable to the
314 dissociation of highly excited molecules. Concerning clusters of different charge states, we have
315 some information about the energy deposited by electron capture (q=0) and by ionization (q⩾2)
316 [33, 41] but no indication at all as to the type of molecular states that are populated. Then again
317 the number of molecular states considered in a counting may be much too large. Possible directions
318 could be to look at the *individual* ion pair dissociation channels and associated branching ratios
319 within a given (n,q) species that have not been exploited so far (only the total probability was here

₃₂₀ discussed). Also it could be of interest to compare to IPD in other systems. We recently measured
₃₂₁ IPD in C_nN^+ clusters instead of C_n^+ projectiles. The first results for $n = 1$ indicate sizeably
₃₂₂ lower IPD rates for identical electron capture, dissociative electronic excitation and ionization
₃₂₃ cross sections. The whole n series ($n = 1 - 4$) will be studied and analysed in the near future.

Appendix: Group theoretical treament

₃₂₉   This appendix explains the group theoretical treatment which has been used for deriving the
₃₃₀ type and respective number of molecular states correlating to ion pair dissociation channels reported
₃₃₁ in Tables II and III. The procedure will first be presented using C_2^+ as an example. It will then be
₃₃₂ applied to linear C_3^+ in which two different coupling cases occur.

1. $\mathbf{C^-(^4S^\circ) + C^{2+}(^3P^\circ) \longrightarrow C_2^+}$
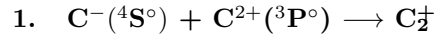
₃₃₄   Applying the Wigner-Witmer diatomic correlation rules for unlike atomic fragments C^- and
₃₃₅ C^{2+} (see Table 26 of Herzberg book [35]), and performing the spin coupling leads to the resulting
₃₃₆ $C_{\infty v}$ molecular states :

$$^2\Sigma^-, ^2\Pi, ^4\Sigma^-, ^4\Pi, ^6\Sigma^-, ^6\Pi, \tag{A.1}$$

₃₃₇   Note that for spatial symmetry the same result is obtained from a direct product adapted to
₃₃₈ $C_{\infty v}$ symmetry : $\Sigma^-(S^\circ)$ x $(\Sigma^+ + \Pi)$ $(P^\circ) \to \Sigma^- + \Pi$.
₃₃₉ The results (A.1) do not take however into account the fact that, while fragments with different
₃₄₀ numbers of electrons are unlike, they have nevertheless identical nuclei. It follows that C_2^+ is an
₃₄₁ homonuclear system possessing $D_{\infty h}$ inversion symmetry. As inversion transforms a function cen-
₃₄₂ tred on one nucleus to the same function on the other one, it is necessary to build the eigenfunctions
₃₄₃ of C_2^+ at dissociation limit as linear combinations of the two degenerate wavefunctions differing by
₃₄₄ a permutation of the two identical carbon nuclei numbered 1 and 2 :

$$\Psi_{\pm} = \frac{1}{\sqrt{2}}[\Psi(C^-(^4S^\circ);1) \times \Psi(C^{2+}(^3P^\circ);2)] \pm [\Psi(C^-(^4S^\circ);2) \times \Psi(C^{2+}(^3P^\circ);1)] \quad \text{(A.2)}$$

These functions maintain the spin and $C_{\infty v}$ characters of (A.1), but are also eigenfunctions of the molecular inversion operator, with characters g and u for Ψ_+ and Ψ_-, respectively. The final result is thus :

$$C^-(^4S^\circ) + C^{2+}(^3P^\circ) \longrightarrow {}^2\Sigma_g^-, {}^2\Pi_g, {}^4\Sigma_g^-, {}^4\Pi_g, {}^6\Sigma_g^-, {}^6\Pi_g \text{ and } {}^2\Sigma_u^-, {}^2\Pi_u, {}^4\Sigma_u^-, {}^4\Pi_u, {}^6\Sigma_u^-, {}^6\Pi_u \quad \text{(A.3)}$$

among which only some of the states obey to the selection rules (see Table II).

2. $C^-(^4S^\circ) + C^+(^2P^\circ) + C^+(^4P) \longrightarrow C_3^+$

All participating ion pair dissociation limits of C_3^+ correspond to $C^-/\,C^+/\,C^+$ channels, and in the present case the two identical C^+ fragments are in different electronic states. As in the case of C_2^+, while fragments C^- and C^+ are unlike, molecular states arise from three identical carbon nuclei and belong to the $D_{\infty h}$ point group. Note that the middle fragment is centred at the inversion point and already possess the molecular g/u symmetry.

Six degenerate uncoupled fragments wavefunctions can be built, each differing by a permutation of the three identical carbon nuclei :

$$\Psi_{ijk} = \Psi(C^-(^4S^\circ);i) \times \Psi(C^+(^2P^\circ);j) \times \Psi(C^+(^4P);k) \quad \text{(A.4)}$$

with ijk= $123, 213, 132, 231, 312$ and 321, defining the numbering of the nuclei.

The total degeneracy of this channel is very high ($6 \times 288 = 1728$). Each wavefunction in (A.4) leads to the same resulting $C_{\infty v}$ states, resulting from the $C_{\infty v}$ adapted direct product or from the Wigner-Witmer rules extended to linear polyatomic molecules (see Table 22 of Herzberg [36]) :

$$^{2,4,6}[\Sigma^+(4), \Sigma^-(2), \Pi(4), \Delta(2)] +^8 [\Sigma^+(2), \Sigma^-(1), \Pi(2), \Delta(1)] \quad \text{(A.5)}$$

Eigenfunctions of the molecular inversion operator are obtained by projecting (A.4) functions on the irreducible representations (IRs) A_g and A_u of the inversion group C_i, leading to linear combinations of 3 couples of Ψ_{ijk} functions :

$$\Psi_{1\pm} = \frac{1}{\sqrt{2}}[\Psi_{123} \pm \Psi_{321}]$$

$$\Psi_{2\pm} = \frac{1}{\sqrt{2}}[\Psi_{132} \pm \Psi_{312}] \tag{A.6}$$

$$\Psi_{3\pm} = \frac{1}{\sqrt{2}}[\Psi_{213} \pm \Psi_{231}]$$

For all of these eigenfunctions, the symmetric and antisymmetric products of the atomic functions on nuclei 1 and 3 are g and u, respectively, but the function on the central nucleus 2 is g or u, depending of its atomic parity. It follows that Ψ_{1-}, Ψ_{2+}, Ψ_{3-} are g and Ψ_{1+}, Ψ_{2-} and Ψ_{3+} are u. The final result is that all $C_{\infty v}$ of Eq. A.5 occur 3 times with g and three times with u symmetry. States meeting the selection rule are $^2\Sigma_g^+(12)$ and $^2\Pi_g(12)$.

3. $\mathbf{C^-(^4S^\circ) + C^+(^2P^\circ) + C^+(^2P^\circ) \longrightarrow C_3^+}$

The second case to consider for C_3^+ is when both C^+ ions are in the same state. Only three different degenerate uncoupled fragments wavefunctions appear in this case (identical C^+ are not exchanged):

$$\Psi_{ijk} = \Psi(C^-(^4S^\circ);i) \times \Psi(C^+(^2P^\circ);j) \times \Psi(C^+(^2P^\circ);k) \tag{A.7}$$

with ijk= 123, 213 and 321.

The projection of (A.7) functions on IRs of C_i tell us that Ψ_{123} already belongs to $D_{\infty h}$ and that a linear combination is formed with the two remaining functions:

$$\Psi_{\pm} = \frac{1}{\sqrt{2}}[\Psi_{123} \pm \Psi_{321}] \tag{A.8}$$

$C_{\infty v}$ states arising from Ψ_{123} or Ψ_{321} are obtained as before from Herzberg Tables [36] :

$$^2[\Sigma^+, \Sigma^-(2), \Pi(2), \Delta], ^4[\Sigma^+(2), \Sigma^-, \Pi(4), \Delta(2)], ^6[\Sigma^+, \Sigma^-(2), \Pi(2), \Delta] \tag{A.9}$$

All these states exist with additional g and u characters for Ψ_- and Ψ_+, respectively.

States of $D_{\infty h}$ symmetry resulting from Ψ_{213} do not occur in g,u pairs. The group theoretical treatment is different from previous ones. One must first couple both identical fragments together using the same rules as those applying to an homonuclear diatomic molecule formed from identical $^2P^\circ$ states (see Table 28 of [35]) :

$$^1[\Sigma_g^+(2), \Sigma_u^-, \Pi_g, \Pi_u, \Delta_g], ^3[\Sigma_u^+(2), \Sigma_g^-, \Pi_g, \Pi_u, \Delta_u] \tag{A.10}$$

382 Noting that the g and u symmetry is governed by the antisymmetry of the total electronic
383 eigenfunctions including the spin part. All states of (A.10) must then be coupled to the $^4\text{S}^\circ$ state
384 of C$^-$, which transforms to $^4\Sigma_u^-$ symmetry under $C_{\infty v}$ transformation, leading to:

$$^{2,4,6}[\Sigma_g^-(2), \Sigma_u^+, \Pi_g, \Pi_u, \Delta_g], {}^4[\Sigma_u^-(2), \Sigma_g^+, \Pi_g, \Pi_u, \Delta_u] \tag{A.11}$$

385 States arising from the C$^-$($^4\text{S}^\circ$) + C$^+$($^2\text{P}^\circ$) + C$^+$($^2\text{P}^\circ$) channel result from the sum of (A.9)
386 g,u pairs and (A.11), from which only one $^2\Sigma_g^+$ and three $^2\Pi_g$ states meet the selection rule.

[1] R. Locht and J. Momigny, International Journal of Mass Spectrometry and Ion Physics **7**, 121 (1971).

[2] A. G. Suits and J. W. Hepburn, Annual Review of Physical Chemistry **57**, 431 (2006).

[3] M. J. Simpson and R. P. Tuckett, International Reviews in Physical Chemistry **30**, 197 (2011).

[4] S. X. Tian, Phys. Chem. Chem. Phys. **14**, 6433 (2012).

[5] W. Zong, G. H. Dunn, N. Djurić, M. Larsson, C. H. Greene, A. Al-Khalili, A. Neau, A. M. Derkatch, L. Vikor, W. Shi, A. Le Padellec, S. Rosén, H. Danared, and M. af Ugglas, Phys. Rev. Lett. **83**, 951 (1999).

[6] O. Yenen, D. H. Jaecks, and L. M. Wiese, Phys. Rev. A **39**, 1767 (1989).

[7] M. Farizon, N. V. de Castro Faria, B. Farizon-Mazuy, and M. J. Gaillard, Phys. Rev. A **45**, 179 (1992).

[8] M. Barbatti, L. P. G. de Assis, G. Jalbert, L. F. S. Coelho, I. Borges, and N. V. de Castro Faria, Phys. Rev. A **59**, 1988 (1999).

[9] J. Tabet, S. Eden, F. Gobet, B. Farizon, M. Farizon, S. Ouaskit, P. Scheier, and T. D. Märk, International Journal of Mass Spectrometry **272**, 48 (2008).

[10] J.-Y. Chesnel, Z. Juhász, E. Lattouf, J. A. Tanis, B. A. Huber, E. Bene, S. T. S. Kovács, P. Herczku, A. Méry, J.-C. Poully, J. Rangama, and B. Sulik, Phys. Rev. A **91**, 060701 (2015).

[11] G. Dujardin, L. Hellner, B. J. Olsson, M. J. Besnard-Ramage, and A. Dadouch, Phys. Rev. Lett. **62**, 745 (1989).

[12] E. Rühl and R. Flesch, The Journal of Chemical Physics **121**, 5322 (2004).

[13] L. H. Coutinho, D. J. Gardenghi, A. S. Schlachter, G. G. B. de Souza, and W. C. Stolte, The Journal of Chemical Physics **140**, 024314 (2014).

[14] W. C. Stolte, M. M. Sant'Anna, G. Öhrwall, I. Dominguez-Lopez, M. N. Piancastelli, and D. W. Lindle, Phys. Rev. A **68**, 022701 (2003).

[15] A. V. Baklanov, L. M. C. Janssen, D. H. Parker, L. Poisson, B. Soep, J.-M. Mestdagh, and O. Gobert, Journal of Chemical Physics **129** (2008), 10.1063/1.3026613.

[16] S. M. Poullain, K. Veyrinas, P. Billaud, M. Lebech, Y. J. Picard, R. R. Lucchese, and D. Dowek, The Journal of Chemical Physics **139**, 044311 (2013).

[17] C. Elkharrat, Y. J. Picard, P. Billaud, C. Cornaggia, D. Garzella, M. Perdrix, J. C. Houver, R. R. Lucchese, and D. Dowek, J. Phys. Chem. A **114**, 9902 (2010).

[18] K. Béroff, M. Chabot, G. Martinet, T. Pino, S. Bouneau, A. L. Padellec, G. Féraud, N. D. Thi, F. Calvo, C. Bordas, and F. Lépine, J. Phys. B: At. Mol. Opt. Phys. **46**, 015201 (2013).

[19] K. Wohrer, M. Chabot, R. Fossé, and D. Gardès, Review of Scientific Instruments **71**, 2025 (2000).

[20] M. Chabot, S. Della Negra, L. Lavergne, G. Martinet, K. Wohrer-Béroff, R. Sellem, R. Daniel, J. Le Bris, G. Lalu, D. Gardès, J. A. Scarpaci, P. Désesquelle, and V. Lima, Nuclear Instruments and Methods in Physics Research Section B: Beam Interactions with Materials and Atoms **197**, 155 (2002).

[21] M. Chabot, G. Martinet, K. Beroff, T. Pino, S. Bouneau, B. Genolini, X. Grave, K. Nguyen, C. le Gail-

liard, P. Rosier, G. Feraud, H. Friha, and B. Villier, Review of Scientific Instruments **82** (2011), 10.1063/1.3640411.

[22] Jallat PHD thesis University Paris Sud (2015) and to be published.

[23] S. Díaz-Tendero, G. Sánchez, P.-A. Hervieux, M. Alcamí, and F. Martín, Brazilian Journal of Physics **36**, 529 (2006).

[24] S. S. G. Tesina, unpublished , University of Madrid (2006).

[25] J. C. Rienstra-Kiracofe, G. S. Tschumper, H. F. Schaefer, S. Nandi, and G. B. Ellison, Chem. Rev. **102**, 231 (2002).

[26] Barriers of some eV may be present in multicharged species [42, 43].

[27] Convergence problems precluded to reach the real ion pair states; those states have been approximated by an attractive Coulomb potential in this region as often done.

[28] H.-J. Werner, P. J. Knowles, G. Knizia, F. R. Manby, and M. Schütz, WIREs Comput Mol Sci **2**, 242 (2012).

[29] L. H. Toburen, R. D. DuBois, C. O. Reinhold, D. R. Schultz, and R. E. Olson, Phys. Rev. A **42**, 5338 (1990).

[30] K. Beroff, N. T. Van-Oanh, M. Chabot, T. Tuna, T. Pino, G. Martinet, A. Le Padellec, Y. Carpentier, and L. Lavergne, Physical Review A **84** (2011), 10.1103/PhysRevA.84.032705.

[31] K. Wohrer, M. Chabot, J. P. Rozet, D. Gard'es, D. Vernhet, D. Jacquet, S. D. Negra, A. Brunelle, M. Nectoux, M. Pautrat, Y. L. Beyec, P. Attal, and G. Maynard, Journal of Physics B: Atomic, Molecular and Optical Physics **29**, L755 (1996).

[32] M. Chabot and et al., Proceedings of the XXIV ICPEAC , 607 (2006).

[33] K. Béroff, M. Chabot, F. Mezdari, G. Martinet, T. Tuna, P. Désesquelles, A. LePadellec, and M. Barat, Nuclear Instruments and Methods in Physics Research Section B: Beam Interactions with Materials and Atoms Proceedings of the Seventh International Symposium on Swift Heavy Ions in Matter, **267**, 866 (2009).

[34] E. Merzbacher, NATO Courses ASI Series B: Physics, Vol.103, 1983.

[35] G. Herzberg, *Molecular Spectra and Molecular Structure, I. Spectra of Diatomic Molecules* (Van Nostrand Rheinhold, Princeton, New Jersey, 1950).

[36] G. Herzberg, *Molecular Spectra and Molecular Structure III. Electronic Spectra and Electronic Structure of Polyatomic Molecules* (Van Nostrand Rheinhold, Princeton, New Jersey, 1966).

[37] A. Kramida, Yu. Ralchenko, J. Reader, and and NIST ASD Team, NIST Atomic Spectra Database (ver. 5.3), [Online]. Available: `http://physics.nist.gov/asd` [2016, July 11]. National Institute of Standards and Technology, Gaithersburg, MD. (2015).

[38] J. A. Schiavone, S. M. Tarr, and R. S. Freund, J. Chem. Phys. **70**, 4468 (1979).

[39] A. Ehresmann, P. V. Demekhin, W. Kielich, I. Haar, M. A. Schlueter, V. L. Sukhorukov, and H. Schmoranzer, Journal of Physics B-Atomic Molecular and Optical Physics **42** (2009), 10.1088/0953-4075/42/16/165103.

[40] C_2^+ is formed by stripping, at the accelerator terminal, of two electrons from C_2^-. Removing of the two more external electrons from C_2^- (Ground State) leads to $C_2^+(a^2\Pi_u)$.

[41] M. Chabot, G. Martinet, F. Mezdari, S. Diaz-Tendero, K. Béroff-Wohrer, P. Désesquelles, S. Della-Negra, H. Hamrita, A. LePadellec, T. Tuna, L. Montagnon, M. Barat, M. Simon, and I. Ismaïl, J. Phys. B: At. Mol. Opt. Phys. **39**, 2593 (2006).

[42] H. Hogreve, J. Chem. Phys. **102**, 3281 (1995).

[43] H. Hogreve, Journal of Molecular Structure-Theochem **532**, 81 (2000).